Transactions of the American Fisheries Society 150:8–23, 2021

ISSN: 0002-8487 print / 1548-8659 online
DOI: 10.1002/tafs.10270

FEATURED PAPER

Climate, Fire Regime, Geomorphology, and Conspecifics Influence the Spatial Distribution of Chinook Salmon Redds

Gregory R. Jacobs*
River Basin Center, Odum School of Ecology, University of Georgia, Athens, Georgia 30602, USA

Russell F. Thurow
U.S. Forest Service, Rocky Mountain Research Station, Salmon, Idaho 83467, USA

John M. Buffington and Daniel J. Isaak
U.S. Forest Service, Rocky Mountain Research Station, Boise, Idaho 83702, USA

Seth J. Wenger
River Basin Center, Odum School of Ecology, University of Georgia, Athens, Georgia 30602, USA

Abstract

Pacific salmon spawning and rearing habitats result from dynamic interactions among geomorphic processes, natural disturbances, and hydro-climatological factors acting across a range of spatial and temporal scales. We used a 21-year record of redd locations in a wilderness river network in central Idaho, USA, to examine which covariates best predict the spawning occurrence of Chinook Salmon *Oncorhynchus tshawytscha* and how shifts under a changing climate might affect habitat availability. We quantified geomorphic characteristics (substrate size, channel slope, and valley confinement), climatic factors (stream temperature and summer discharge), wildfire, and conspecific abundance (as inferred by the number of redds) throughout the network. We then built and compared logistic regression models that estimated redd occurrence probability as a function of these covariates in 1-km reaches throughout the network under current and projected climate change scenarios. Redd occurrence was strongly affected by nearly all of the covariates examined. The best models indicated that climate-driven changes in redd occurrence probabilities will be relatively small but spatially heterogeneous, with warmer temperatures increasing occurrence probabilities in cold, high-elevation reaches and decreasing probabilities in warm, low-elevation reaches. Furthermore, positive effects of wildfire on redd occurrence may be more important than climate-driven effects on stream temperature and summer discharge, although climate-related changes in temperature and scour regime during the egg incubation period may influence survival to emergence. Our results identify where favorable spawning habitats are likely to exist under climate change, how future habitat distributions may differ from contemporary conditions, and where habitat conservation might be prioritized. Furthermore, the positive occurrence–abundance relationship we observed indicates that the study site is underseeded, and effective management actions are needed for increasing the recruitment of spawning adults to take advantage of available habitat.

After European settlement, the distribution and abundance of salmon *Oncorhynchus* spp. and steelhead *O. mykiss* in the Pacific Northwest of North America declined due to habitat degradation, migration barriers, overharvest, and interactions with nonnative fishes (NRC 1996; Lee 1997). Subsequent recovery efforts have been

*Corresponding author: grjacobs@gmail.com
Received April 20, 2020; accepted September 3, 2020

manifold and expensive, including protection under the Endangered Species Act of 1973 and the investment of mitigation funding from major hydroelectric dam projects (NPCC 2019). However, broad salmon recovery has remained elusive, with many populations persisting at abundances far below historical levels (Thurow et al. 2020). Moving forward, successful conservation will require careful spatial prioritization based on the distribution and abundance of suitable habitat, especially habitat used for spawning (Isaak and Thurow 2006; Peterson et al. 2013).

Mature salmon migrate from the ocean to their natal freshwater streams, where adult females excavate streambed nests (redds) in which the adults spawn and the fertilized eggs develop. The quality of salmon spawning and rearing habitat is affected by a variety of physical factors, including channel morphology, stream temperature, flow depth, velocity, hyporheic flow, and substrate size (e.g., Beechie et al. 2008). Egg development and fry survival are sensitive to the degree of fine-sediment infiltration (Chapman 1988; Jensen et al. 2009), scouring flows (Montgomery et al. 1996), water temperature (Richter and Kolmes 2005), and oxygen concentration as influenced by hyporheic exchange (Greig et al. 2007; Tonina and Buffington 2009). Where natural fire regimes are intact, wildfire may contribute new and transient high-quality habitat patches resulting from periodic post-fire debris flows that recruit wood and sediment from upstream watersheds (Flitcroft et al. 2016), despite short-term negative effects on stream habitat (Minshall et al. 1990; Minshall 2003). Climate change is altering many of these factors (Luce et al. 2013; Jolly et al. 2015; Isaak et al. 2018), producing shifts in species distributions (Lynch et al. 2016) that can challenge conservation efforts focused on current habitat distributions. Increasing water temperatures are predicted to cause habitat loss for stream fishes as lower-elevation areas warm (Lynch et al. 2016), although in some cases those losses can be offset by warming of upstream sites that were previously below thermal optima (Isaak et al. 2016). In addition, climate change can alter stream habitat quality due to changes in streamflow regime (Wenger et al. 2011) and disturbances associated with fire and debris flows (Goode et al. 2012; Flitcroft et al. 2016).

A complicating factor is that salmon habitat use may vary depending on the abundance of annually returning salmon, which is affected by out-of-basin factors, such as ocean productivity and migration mortality (Crozier et al. 2019). Female salmon are territorial, so during years with higher adult returns, breeding expands into previously unoccupied sites (Isaak and Thurow 2006). Thus, variation in conspecific density may shift occupancy–environment relationships (Falcy 2015).

Although the effects of many covariates on salmon are well established in isolation, their relative importance and joint effects in driving variation in spawning distributions across landscapes are less well established. Probabilistic species distribution models are powerful tools for assessing the joint effects of covariates, quantifying the roles of habitat conditions on species, and predictively mapping occurrence probabilities across large domains (Elith and Leathwick 2009). Coupling species distribution models with large data sets from ongoing monitoring programs (e.g., Roper et al. 2019; Thurow et al. 2020) and improved geospatial representations of stream habitat (Hill et al. 2016; Isaak et al. 2017) creates new opportunities to better quantify salmon habitat relationships and to understand or plan for the effects of climate change.

In this study, we examined the distribution of Chinook Salmon *O. tshawytscha* redds throughout the Middle Fork Salmon River (MFSR) in central Idaho (Figure 1). The MFSR populations of Chinook Salmon were first listed as "threatened" under the Endangered Species Act in 1992 (NOAA 1992) and have been the focus of extensive recovery efforts. Several physical and biological research programs have produced detailed geospatial data sets for the MFSR basin that can be used to evaluate redd occurrence as a function of environmental conditions over space and time. The MFSR is relatively unaltered by humans and hosts an almost exclusively wild (albeit depleted) Chinook Salmon population (Thurow et al. 2020). Hundreds of kilometers of intact Chinook Salmon spawning streams flow through the MFSR watershed, the bulk of which occurs within the Frank Church River of No Return Wilderness (Thurow et al. 2020). Our goal was to model the relationships between Chinook Salmon spawning locations and habitat covariates across a range of interannual variation in spawner abundance for all accessible stream reaches in the MFSR. After developing models to describe those relationships, we used the models to predict redd occurrence probabilities and assessed the potential effects of changes in summer stream temperature and discharge under two future climate scenarios.

METHODS

Redd surveys.— Annually from 1995 through 2015, individual redd locations were georeferenced with a GPS unit at the end of the spawning season. Redd surveys were conducted via low-altitude helicopter flights (Thurow 2000) supplemented by ground-based surveys conducted by a collaborative group of experienced biologists with the Idaho Department of Fish and Game (IDFG), Shoshone–Bannock Tribes, Nez Perce Tribe, and U.S. Forest Service (USFS). Together, these surveys employed a spatially continuous sampling design (Fausch et al. 2002) replicated annually along a 777-km subset of the MFSR stream network, encompassing all potential Chinook Salmon spawning habitats within the 7,330-km^2 MFSR watershed (Figure 1). Streams that were deemed

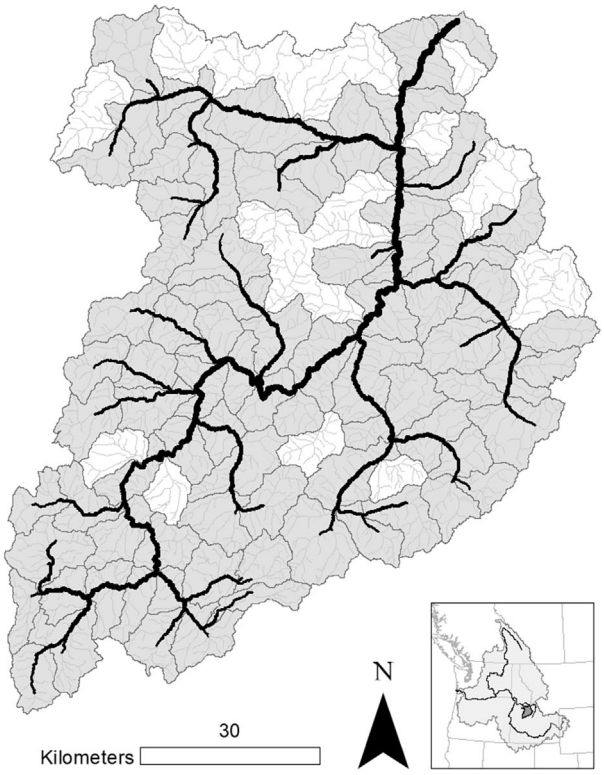

FIGURE 1. Map of the Middle Fork Salmon River (MFSR) in central Idaho. The 1:100,000-scale stream reaches are shown in light gray (Nagel et al. 2017), with reaches surveyed annually for Chinook Salmon redds overlain in black, where line width scales with the log of upstream drainage area. Gray polygons represent 12-digit hydrologic unit code subbasins that overlap the surveyed portion of the stream network; white polygons are areas that do not overlap. Overall, 772 individual reaches comprise the surveyed (black) network. The inset map (39–54°N, 105–126°W) shows the location of the MFSR watershed (dark-gray polygon) within the Columbia River basin (light-gray polygon), with major tributaries, including the upper Columbia, Snake, and Salmon rivers, drawn in black.

inaccessible to Chinook Salmon due to small size and steep slopes were omitted from the survey area (Thurow 2000; Isaak and Thurow 2006). The resulting multi-decadal Chinook Salmon redd database is unique in its combination of fine spatial detail and large spatial and temporal extent. Georeferenced redd locations were snapped to the stream network depicted on the 1:100,000-scale National Stream Internet (Nagel et al. 2017), which divides the network at confluences with further division into approximately 1-km reaches (stream reaches in our network averaged 1 km in length, with an SD of 0.7 km). Each reach was classified by the presence or absence of redds during each year.

Geomorphic covariates.— Redd occurrence was considered in relation to three geomorphic characteristics: median substrate size (D_{50}), channel slope (S), and valley confinement (V). Spatial variation in substrate size within and between stream reaches is a primary control on spawning habitat because the size of sediment that a female salmon can move while excavating a redd is limited by her body size (Kondolf and Wolman 1993); conversely, substrate that is too fine provides poor habitat for egg and fry survival (Chapman 1988; Jensen et al. 2009). Consequently, we hypothesized that Chinook Salmon redd occurrence would exhibit a unimodal relationship with substrate size, indicating an optimal value and avoidance of finer or coarser substrates. Median substrate size was used as a first-order estimate of bed material in each reach, although it is recognized that the extent of suitable spawning substrate additionally depends on the SD of the substrate size distribution (and thus the amount of unsuitable coarse/fine material) (Riebe et al. 2014) and the degree to which the reach is organized into textural patches (mesoscale substrate heterogeneity) (Buffington and Montgomery 1999). River slope is another primary geomorphic control on salmonid spawning habitat because lower stream slopes (<3%) are characterized by gravel- and cobble-bed streams that have beneficial fine-scale habitat conditions, while steeper, boulder-bed streams are generally avoided (Montgomery et al. 1999). Consequently, we expected a negative relationship between Chinook Salmon redd occurrence and S. The third geomorphic control on spawning habitat is valley confinement, which is the lateral extent of the valley floor and floodplain adjacent to the stream. Chinook Salmon in the study area commonly spawn in unconfined valleys (Isaak and Thurow 2006; Goode et al. 2013) because of (1) extensive floodplains that allow overbank flooding, which reduces mortality of incubating embryos from streambed scour (Goode et al. 2013; McKean and Tonina 2013); (2) off-channel habitat that provides refuge during rearing; (3) complex hyporheic exchange and associated benefits during incubation (Baxter and Hauer 2000); and (4) lower-gradient channels that contain more extensive habitat patches than steeper, confined reaches (Stanford et al. 2005). Thus, we hypothesized that Chinook Salmon redds would be more likely to occur in unconfined reaches. We also hypothesized that V would modify the effects of other covariates; specifically, we expected stronger effects of D_{50} on redd occurrence in unconfined valleys because of other beneficial characteristics of such environments, as described above.

We predicted reach-average D_{50} values from a 10-m digital elevation model (USGS 2006) following the methods of Buffington et al. (2004) tailored to field data obtained from 120 sites in the basin. Stream reaches and slopes were defined between 12.192-m (40-ft) contour crossings on 1:24,000-scale topographic maps, with digital stream lines obtained from the National Hydrography Dataset (USGS 2010). Reach average D_{50} and S were thus

determined for stream segments of variable length ranging from less than 100 m to several kilometers depending on the frequency of contour crossings. Overlap of the 1-km reaches with buffer polygons derived from the above 1:24,000-scale network of variable segment lengths was used to calculate average (weighted by overlapping stream length) S and D_{50} values for each 1-km reach. Valley confinement was predicted from the approach of Nagel et al. (2014) and used to determine the proportion of each 1-km reach that ran through unconfined valleys. Valley confinement was treated as a binary variable, wherein 1-km reaches overlapping unconfined valleys by more than 50% of their length were considered "unconfined" ($V = 1$). The three geomorphic covariates (D_{50}, S, and V) were spatially variable but temporally constant in our analysis.

Climate covariates.— We considered the effects of stream temperature (T) and summer discharge (Q; a surrogate for wetted stream width) on the occurrence of redds within reaches. Because MFSR streams occur at high elevation and span a wide range of temperatures, Chinook Salmon habitat suitability may be limited by cold temperatures at high elevations and warm temperatures at low elevations (range = 4.4–17.8°C; Richter and Kolmes 2005). Similarly, stream size may impose physical limits on spawning habitat availability; small streams (e.g., bankfull width <8 m; Isaak and Thurow 2006) will be inaccessible to large-bodied adult Chinook Salmon, whereas large streams may have unfavorable hydraulic conditions for spawning (e.g., Moir et al. 2006). Consequently, we hypothesized that redd occurrence would exhibit a unimodal relationship with both stream temperature and summer discharge, indicating an intermediate optimum for spawning.

To represent contemporary spatial variation in T, we used a pre-existing stream temperature scenario quantifying mean August stream temperatures for 1993–2011 (Isaak et al. 2017), which was downloaded from the NorWeST Web site (https://www.fs.fed.us/rm/boise/AWAE/projects/NorWeST.html). To represent interannual variation in stream temperature, we calculated the deviation (ΔT) of each year's predicted mean August temperature from the 1993–2011 average and applied this deviation to all reaches in that year. The annual difference from the study-wide mean August temperature (i.e., ΔT) ranged from −0.7 to 0.9°C, with a mean of 0°C and an SD of 0.5°C. Since reaches on the cold-edge (or warm-edge) margins would be more (or less) likely to support redds in warmer years, we considered an interaction between T and ΔT in the model.

To represent contemporary spatial variation in Q, we used a pre-existing streamflow scenario representing mean summer discharge for 1977–1997 (Wenger et al. 2010), which was downloaded from the Western U.S. Stream Flow Metrics Web site (USFS, Rocky Mountain Research Station [RMRS]; https://www.fs.fed.us/rm/boise/AWAE/projects/modeled_stream_flow_metrics.shtml). "Summer" was defined as the time period between (1) the first day after June 1 when flows were lower than the mean annual value for the reach and (2) September 30 (Wenger et al. 2010). This streamflow variable (used as a surrogate for wetted stream size at the onset of spawning) varied spatially among the 1-km stream reaches but was a constant during the survey period.

Fire covariates.— We hypothesized that fires in the local area surrounding each reach would initially degrade spawning habitat due to decreased water quality (input of ash and fine sediment) and elevated stream temperatures (loss of vegetative shading) but that habitat would improve in subsequent years due to an input of spawning gravels and wood from post-fire debris flows. We focused on local effects (5-km local watershed) because the effects of post-fire debris flows are most pronounced at subbasin confluences (where debris fans form) and within the first several kilometers downstream of the confluence as the pulse of gravel and wood disperses (Benda et al. 2003; M. Lewicki, U.S. Bureau of Reclamation, J. M. Buffington, R. F. Thurow, and D. J. Isaak, unpublished data). The perimeters of burned areas within the MFSR from 1990 through 2016 were downloaded from the Monitoring Trends in Burn Severity Web site (https://www.mtbs.gov/), which provides data on the burn severity and extent of all large fires in the United States (Eidenshink et al. 2007). We then calculated the proportion of the local watershed area for each reach that had burned within each year. We defined the local watershed as that within a 5-km upstream radius from the center of the reach, from which we produced local watershed polygons using the Geodata Crawler spatial data processing tool (Leasure 2014). We used within-year local watershed burned area as the short-term fire effects variable F_0. For longer-term fire effects, we calculated the sum of the local area burned over moving-window 3- and 5-year periods (F_3 and F_5, respectively). These three local watershed fire variables varied spatially by 1-km reach and temporally by year.

Annual redd abundance.— The numbers of adult Chinook Salmon returning to the MFSR varied by two orders of magnitude among years during the monitoring period, which we hypothesized would influence reach-level redd occupancy probability. To examine how habitat occupancy probability responded to variation in broader-scale redd abundance (an index of spawning run size), we quantified three scales of annually varying redd abundance: the whole MFSR basin (N_{MFSR}); the eight subwatershed-scale populations recognized by the National Oceanic and Atmospheric Administration's Interior Columbia Basin Technical Recovery Team (ICTRT 2003) that overlap our surveyed network (N_{POP}); and the 23 network segments used by Isaak and Thurow (2006) to divide the core

TABLE 1. Summary statistics for all environmental covariates included in Chinook Salmon redd occurrence models (min = minimum; max = maximum). Symbols are defined in the Methods section.

Variable	Mean	SD	Median	Min	Max
D_{50} (mm)	51.3	16.2	49.3	13.6	122.1
$\log_e(D_{50})$	3.884	0.338	3.897	2.607	4.805
S (%)	1.8	1.7	1.3	0.1	16.3
V	0.27	0.45	0	0	1
Q (m^3/s)	272.3	442.4	73.9	2.6	2,001.6
$\log_e(Q)$	4.489	1.516	4.303	0.945	7.602
T (°C)	12.5	2.2	12.6	6.6	17.5
ΔT (°C)	0.0	0.5	−0.2	−0.7	0.9
N_{MFSR} (redds)	816	600	633	20	2,271
N_{POP} (redds)	90	125	43	0	690
N_{SEG} (redds)	36	66	10	0	472
F_0 (km^2)	0.177	1.248	0	0	29.39
F_3 (km^2)	0.512	2.093	0	0	29.39
F_5 (km^2)	0.824	2.611	0	0	29.39

network into roughly equal-sized segments, with divisions placed near major tributary junctions (N_{SEG}). The N_{MFSR} variable represents the hypothesis that occurrence probability varies with redd abundance across the entire MFSR, the N_{POP} variable represents the hypothesis that occurrence probability varies with "regional" abundance of redds in the local (ICTRT 2003) population, and the N_{SEG} variable represents the hypothesis that occurrence probability varies with "local" abundance of redds within the network segments of Isaak and Thurow (2006). We also tested interactions between each abundance covariate and physical characteristics of slope and substrate size.

Model fitting and evaluation.— We used logistic regression models to estimate relationships between environmental covariates (Table 1) and Chinook Salmon redd occurrence within reaches. We identified 20 hypotheses from the variables described above (Supplement S1 available in the online version of this paper). Plausible combinations of these hypotheses comprised a candidate set of 1,080 models that described occurrence probability as a function of landscape habitat covariates (Supplement S2 available in the online version of this paper). We evaluated these model hypotheses using a common random effect structure for all candidate models, where reach-specific deviations from landscape habitat–redd occurrence relationships among 1-km reaches were accounted for by incorporating nested random intercepts for stream reaches within 12-digit hydrologic unit code (HUC-12) subbasins (Figure 1; Seaber et al. 1987). This structure accounted for localized residual spatial autocorrelation within and among HUC-12 subbasins, with each containing between 2 and 24 contiguous surveyed stream reaches (mean = 10.6 reaches; SD = 5.1).

We fit all candidate mixed-effects logistic regression models in R (R Core Team 2019) using maximum likelihood estimation for comparison by Akaike's information criterion (AIC) using the R package glmmTMB to leverage its faster speed over other functions used for mixed-model fitting (Brooks et al. 2017). Models were ranked based on the difference in AIC score between each model i and the best-performing model (i.e., the model with the lowest score, min[AIC]): $\Delta AIC_i = AIC_i - \min(AIC)$. Models with ΔAIC_i less than 10 (our "confidence set") were re-fitted using the R package lme4 (Bates et al. 2015) to leverage that package's internal model-fitting diagnostics and established connections with related R packages. Diagnostic statistics were used to evaluate aspects of model fit that are not described by AIC scores: (1) out-of-sample area under the receiver operating characteristic curve (AUC) statistic, which indicates model prediction performance and transferability; (2) conditional and marginal R^2 values for mixed-effects generalized linear models (Nakagawa et al. 2017), which indicate goodness of fit; (3) Kolmogorov D-statistic, used to test for model missspecification based on the distribution of quantile model residuals from the DHARMa package (Hartig 2019); and (4) Moran's I-statistic, to test for residual spatial autocorrelation (in Euclidean space; Hartig 2019). An 8-fold cross validation routine was performed to calculate the out-of-sample AUC score, with folds stratified by population (ICTRT 2003) to maintain the HUC-based spatial structure in our random effects (sensu Roberts et al. 2017). We evaluated variance inflation factors for parameters in each model in our confidence set but found no evidence of strong collinearity (Fox and Monette 1992). We used empirical Bayesian model averaging—also called prediction averaging (as opposed to parameter averaging)—to combine reach-level predictions from each of the models in our confidence set, weighted by the corresponding AIC weight for that model, using the package MuMIn

(Bartón 2019). We used these model-averaged predictions to describe the relationships between redd occurrence probabilities and covariates by constructing response curves of predictions across the observed ranges of covariate values.

Redd distribution forecasting in a changing climate.— We used the same confidence set of models to evaluate how redd occurrence probabilities across the MFSR network would change under projected future climate scenarios. Although climate is likely to affect a variety of environmental parameters, we focused on changes to T and summer Q, holding other variables constant. Redd occurrence probabilities were predicted for a baseline scenario using contemporary values of those covariates and compared with expectations for 2040 and 2080 based on the Intergovernmental Panel on Climate Change (IPCC 2007) A1B emissions trajectory (Wenger et al. 2010; Isaak et al. 2017). We calculated model-averaged predictions of the reach-specific probability of redd occurrence, unconditional on random effects (i.e., ignoring random effects at the reach and HUC-12 scales) for 2040 and 2080, assuming that other covariates in the final model persisted at the temporal average observed from 1995 to 2015 (e.g., $N_{\mathrm{MFSR}} = 816$ redds; $F_5 = 0.82\ \mathrm{km}^2$; and $F_0 = 0.18\ \mathrm{km}^2$). Other variables in the final model (i.e., D_{50}, S, and V) were invariant within a reach, so we used those reach-specific values in our projections. We also evaluated the predictions under the contemporary climate scenario with ± 1 SD in upstream burned area for the 5-year and within-year events to evaluate the sensitivity of model predictions to fire variation.

To represent variation in habitat suitability across the MFSR for current and future conditions, we defined a relative index of total habitat suitability (H_T) following Wenger et al. (2013) as the sum of the products of stream reach lengths ($L_{[i]}$) and unconditional, model-averaged occurrence probabilities ($\hat{y}_{[i]}$):

$$H_T = \sum_{i=1}^{n} \left[\hat{y}_{(i)} L_{(i)} \right], \tag{1}$$

where i indexes the 772 reaches (~1 km each) in our data set. The index H_T sums the distribution of predicted spawning habitat across the stream network into a summary metric for the basin, contingent on the limitations of our data set, such as low observed escapements (Thurow et al. 2020). We emphasize that H_T is a measure of redd occurrence probability as a function of landscape covariates, dependent on observed Chinook Salmon densities, which we assume to be a reflection of habitat suitability. Furthermore, H_T is a relative index because it is a function of predicted habitat occupancy, which in our model varies annually with the number of returning Chinook Salmon. To visualize how environmental changes may shift the distribution of redds within the basin under a changing climate, we plotted the accumulation of H_T with elevation and distance upstream for contemporary conditions (with and without observed variation in burned area) and for the 2040 and 2080 climate change projections. Additionally, we calculated and plotted elevations and distances where the 5th, 50th, and 95th percentiles of H_T occurred for each scenario. Elevation was measured in meters from sea level, and distance was measured in kilometers upstream from the outlet of the surveyed network.

RESULTS

The final data set consisted of 15,614 presence/absence records (out of a possible 16,212) across the surveyed network over 21 years. We removed 578 records for reaches that were not sampled in years when adverse conditions, such as high winds or wildfire, prohibited helicopter flights over part of the basin or when turbid water from storms and debris flows inhibited redd visibility. We removed 20 additional records that were missing hydrological data. Twelve models had AIC scores within 10 units of the best model, comprising our confidence set (Supplement S2), from which we derived weighted average predictions of redd occurrence. Additional model diagnostics (Table 2) indicated that all models in the confidence set performed well. The AUC scores were all near 0.8, indicating good model fit. Generally high conditional R^2 values near 0.73 indicated that the random effects strongly influenced variation in redd occurrence, but marginal R^2 values near 0.42 showed that main effects also explained a considerable amount of the variation in redd occurrence. The P-values for Kolmogorov–Smirnov D and Moran's I indicated that models were not misspecified, and only one model showed significant residual spatial autocorrelation (model 5: $P[I] = 0.045$).

Covariate Effects

Across our model-averaged predictions, the occurrence of redds was a unimodal function of the mean stream temperature in August (T), reaching its maximum at 13.4°C and declining at higher and lower temperatures (Figure 2A). Interannual temperature variation (ΔT) had no appreciable effect on this relationship. Instead, there was a very slight increase in redd occurrence during years when mean temperatures were higher and a very slight decrease when temperatures were cooler (black versus light-gray curves in Figure 2A), which did not conform to our a priori expectation (Supplement S1). Redd occurrence in confined valleys showed a weak negative response to fire in the short term (within-year effects, F_0) and a positive response to fire during the preceding 5 years (F_5; Figure 2B, C). Results were modulated by valley confinement, with higher probability of redd occurrence in unconfined channels. Redd occurrence in unconfined valleys exhibited a similar short-term response but showed a stronger

TABLE 2. Performance of the 12 best models for predicting the occurrence of Chinook Salmon redds (ΔAIC [difference in Akaike's information criterion] < 10). The coefficient columns specify the modeled fixed effects (symbols are defined in the Methods section); the random effects (random reach nested in 12-digit hydrologic unit code subbasin intercepts) are common to all models we considered. All other columns show diagnostic information for each model: AUC is the area under the receiver operating characteristic curve, calculated from held-out data during an eightfold cross validation analysis; R^2_{cond} and R^2_{marg} are the conditional and marginal R^2 values for mixed-effects generalized linear models (Nakagawa et al. 2017); $P(D)$ is the P-value for the Kolmogorov–Smirnov D-statistic, testing the uniformity in quantile model residuals from the DHARMa package (Hartig 2019); $P(I)$ is the P-value for Moran's I-statistic, testing spatial autocorrelation in Euclidean space (Hartig 2019); ΔAIC is the difference from the lowest AIC in the model set; and w_{AIC} is the AIC weight. Note that squared variables in the column headings (e.g., D^2_{50}) always indicate the full polynomial ($D_{50} + D^2_{50}$), and interactions with these variables (e.g., $D^2_{50} \times N_{\text{MFSR}}$) always indicate an interaction with both terms in the polynomial ($[D_{50} \times N_{\text{MFSR}}] + [D^2_{50} \times N_{\text{MFSR}}]$). See Supplement S1 for hypotheses.

Rank	D^2_{50}	V	T^2	ΔT	Q^2	N_{MFSR}	F_5	F_0	$D^2_{50} \times N_{\text{MFSR}}$	$T^2 \times \Delta T$	$D^2_{50} \times V$	$Q^2 \times V$	$F_0 \times V$	$F_5 \times V$	AUC	R^2_{cond}	R^2_{marg}	$P(D)$	$P(I)$	ΔAIC	w_{AIC}
1	x	x	x	x	x	x	x		x	x	x				0.801	0.726	0.420	0.196	0.458	0.000	0.373
2	x	x	x	x	x	x	x	x	x	x	x				0.801	0.726	0.421	0.189	0.278	0.555	0.283
3	x	x	x	x	x	x	x	x	x	x	x		x		0.801	0.726	0.421	0.192	0.933	1.972	0.139
4	x	x	x	x	x	x	x		x	x	x			x	0.801	0.727	0.420	0.169	0.536	3.795	0.056
5	x	x	x	x	x	x	x		x	x		x		x	0.798	0.731	0.419	0.204	0.045	4.345	0.042
6	x	x	x	x	x	x	x		x	x	x	x		x	0.801	0.728	0.422	0.263	0.672	4.820	0.033
7	x	x	x	x	x	x	x	x	x	x	x			x	0.801	0.727	0.420	0.190	0.212	5.390	0.025
8	x	x	x	x	x	x	x	x	x	x		x		x	0.798	0.731	0.419	0.168	0.726	5.769	0.02
9	x	x	x	x	x	x	x	x	x	x	x	x		x	0.801	0.728	0.423	0.272	0.587	6.792	0.012
10	x	x	x	x	x	x	x	x	x	x	x		x	x	0.801	0.727	0.420	0.197	0.937	7.955	0.007
11	x	x	x	x	x	x	x	x	x	x		x	x	x	0.798	0.731	0.419	0.168	0.928	8.701	0.005
12	x	x	x	x	x	x	x	x	x	x	x	x	x	x	0.801	0.728	0.423	0.263	0.144	9.713	0.003

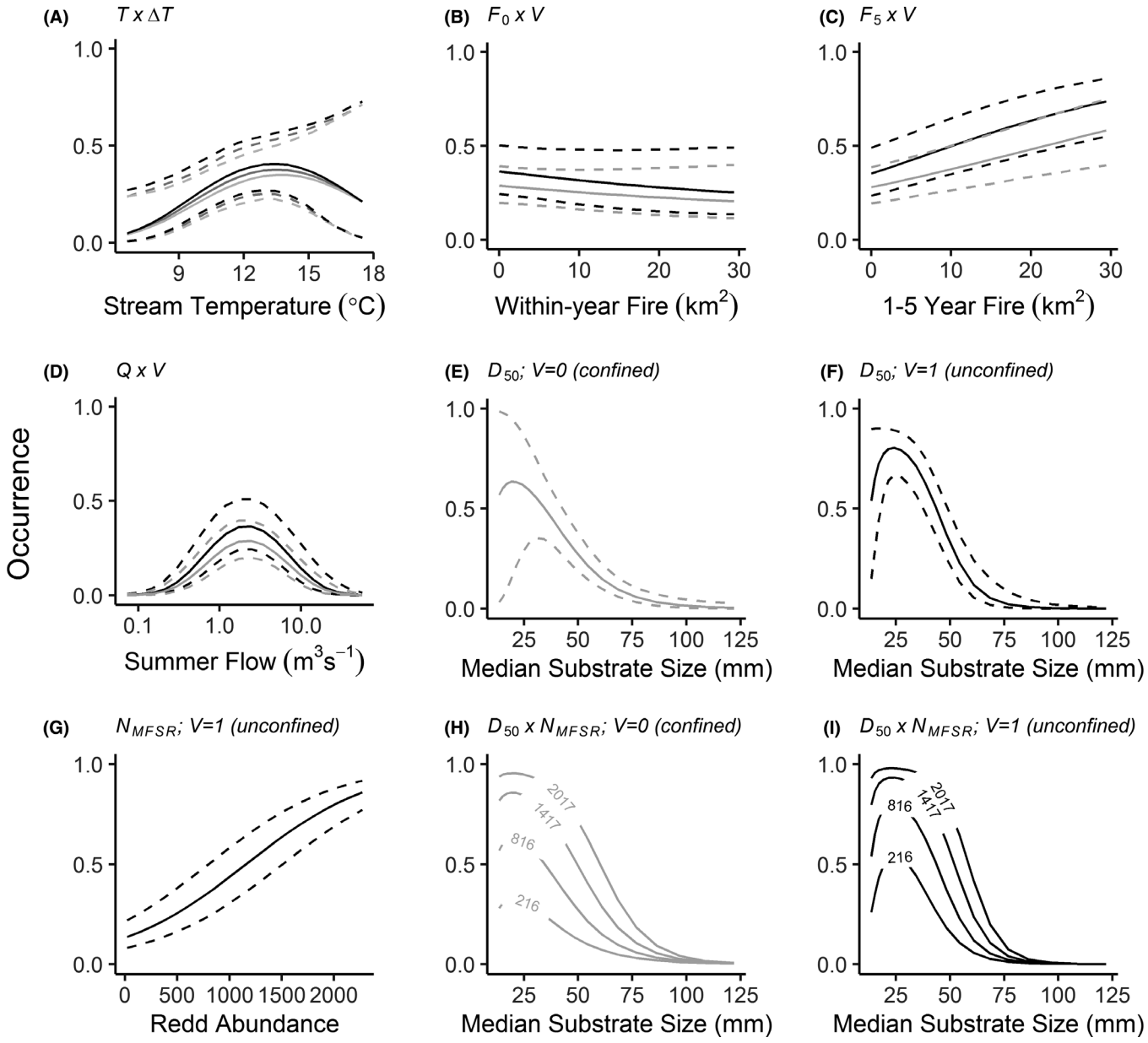

FIGURE 2. Probability of Chinook Salmon redd occurrence as a function of **(A)** stream temperature (T), **(B)** within-year fire extent in the local 5-km watershed (F_0), **(C)** 5-year fire extent in the local watershed (F_5), **(D)** mean summer discharge (Q; a surrogate for wetted stream size during spawning), **(E)** median substrate size (D_{50}) in confined valleys ($V = 0$), **(F)** median substrate size in unconfined valleys ($V = 1$), **(G)** the abundance of redds (N_{MFSR}; year-specific basinwide Chinook Salmon redd count [MFSR = Middle Fork Salmon River]) in unconfined valleys ($V = 1$), **(H)** the influence of redd abundance on the substrate size effect in confined valleys, and **(I)** the influence of redd abundance on the substrate size effect in unconfined valleys. Dashed lines in panels A–G are 95% confidence intervals of the mean (solid lines). Response curves are evaluated at the average of all other covariates, except as indicated by line color or plot labels. Panel A shows responses evaluated at 1 SD below average (light gray), average (dark gray), and 1 SD above average (black) interannual temperature variation. Panels B–I show responses evaluated for confined valleys (gray) and unconfined valleys (black). Panels H and I show responses evaluated at mean redd abundance (816 redds), 1 SD below the mean (216 redds), 1 SD above the mean (1,417 redds), and 2 SDs above the mean (2,017 redds). Note that the lines representing responses at 816 redds in panels H and I are identical to the solid lines in panels E and F, respectively.

positive response to fire during the preceding 5 years (Figure 2B, C). Redd occurrence was also a unimodal function of mean summer Q (a surrogate for wetted stream size during spawning), as expected, reflecting lower suitability of large and small channels compared to an optimum channel size (near 2 m^3/s; Figure 2D).

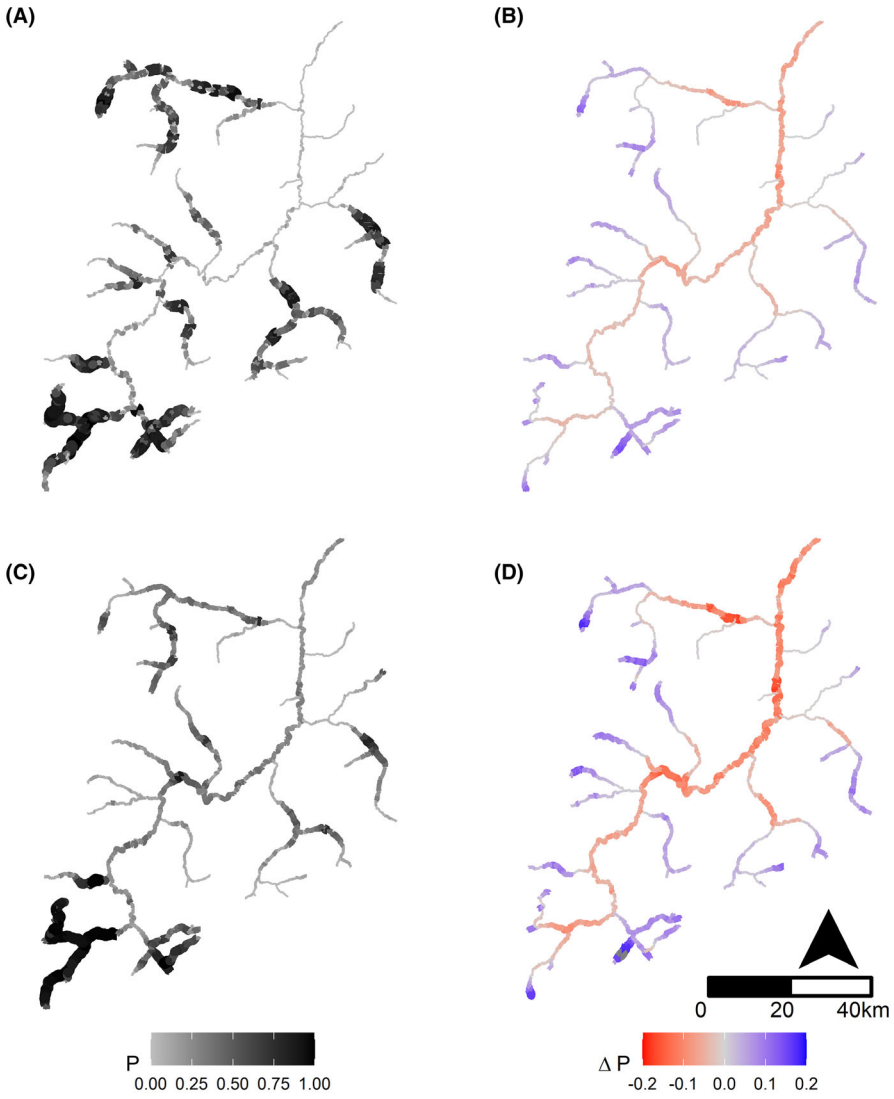

FIGURE 3. Maps describing redd occurrence across potential Chinook Salmon spawning habitats in the Middle Fork Salmon River (MFSR), Idaho: **(A, C)** occurrence probability (P) depicted in terms of the observed proportion of years in which each reach was occupied by redds in the data set (panel A) and model-averaged prediction of P derived from the fixed-effect habitat–redd occurrence relationships in our top models (ignoring spatial random effects) under contemporary environmental conditions (panel C); and **(B, D)** predictions of the change in model-averaged P (ΔP) between contemporary conditions and those under climate change projections for 2040 (panel B) and 2080 (panel D), downscaled to the MFSR from the A1B climate scenario (IPCC 2007). Occurrence probability in panels A and C scales with shading and size, where darker, larger line segments denote higher P. Change in P (ΔP) with climate change is the difference in P between contemporary and projected conditions, such that negative ΔP values indicate predicted reductions in occurrence rate and positive values indicate increases. Values of ΔP in panels B and D scale with size and color from red (20% reduction) to gray (no change) to blue (20% increase).

Reaches were more likely to contain redds if they had D_{50} values near 25 mm (Figure 2E, F). This pattern was qualitatively similar for both confined and unconfined valleys; however, redd occurence in unconfined valleys was more sensitive to variation in substrate size than in confined valleys, and there was a slightly greater predicted probability of redd occurrence in unconfined valleys for the optimal substrate size (D_{50} ≈25 mm; Figure 2E, F). Confined reaches showed substantial uncertainty in the probability of redd occurrence near the optimal substrate size, which attenuated gradually with larger substrate sizes and lower probability of occurrence (Figure 2E). In contrast, unconfined reaches showed a more precise relationship (smaller confidence interval) between redd occurrence and substrate size at smaller D_{50} values (<75 mm; Figure 2F). The inclusion of Chinook Salmon abundance and its

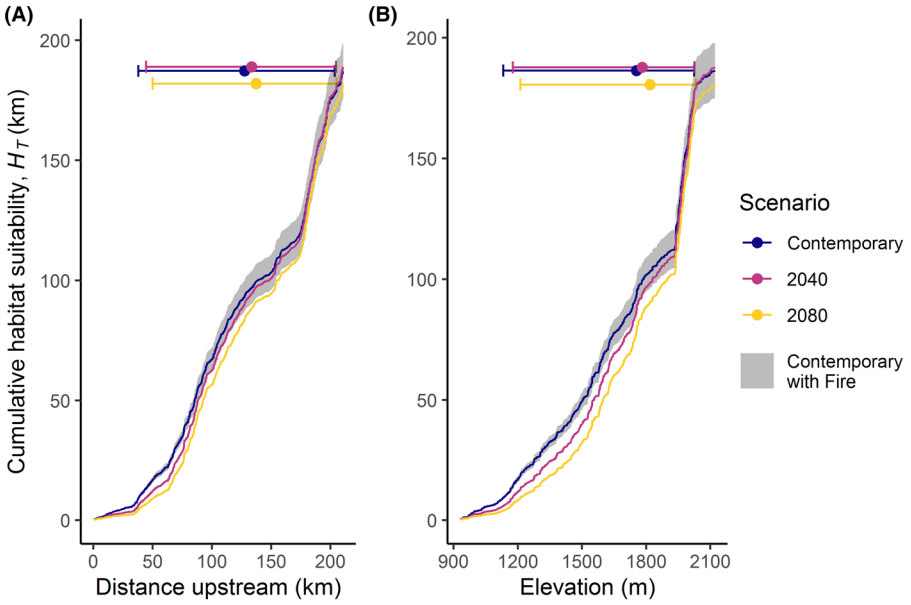

FIGURE 4. Cumulative distributions of H_T (length of stream weighted by the probability of occurrence of Chinook Salmon redds) in the Middle Fork Salmon River as a function of **(A)** distance upstream (km) and **(B)** elevation (m above sea level) for contemporary stream temperatures and mean summer flows (navy blue line) compared to those predicted for 2040 (purple line) and 2080 (gold line) using the A1B climate scenario (IPCC 2007). The gray band around the contemporary curve indicates the prediction space associated with ±1 SD in the within-year (F_0) and 5-year (F_5) fire variables for contemporary conditions, which were used to assess the relative effects of climate-driven changes in stream temperature and streamflow versus variation in fire under current climate conditions. Dot-and-whisker plots at the top of each panel show the location on the *x*-axis of the median and 95th percentile range of H_T, plotted on the *y*-axis at the total cumulative value of H_T for that scenario.

interaction with substrate size in our top models (Table 2) indicated that the probability of redd occurrence for a given reach increased with conspecific abundance (main effect of N_{MFSR}; Figure 2G) and that the increase was largest at substrate sizes below 75 mm ($N_{\mathrm{MFSR}} \times D_{50}$; Figure 2H, I). Importantly, all top models contained the whole-basin-scale conspecific abundance variable, N_{MFSR}, indicating that this variable better explained variation in redd occurrence rates compared to the smaller-scale conspecific abundance variables (N_{POP} and N_{SEG}) that we considered.

Redd Habitat Distribution

We predicted the spatial distribution of Chinook Salmon spawning habitat from our fitted relationships between landscape variables and observed occurrence—without conditioning on our spatial random effects—for contemporary, 2040, and 2080 scenarios. We calculated the weighted average unconditional model predictions from all models in our confidence set by using AIC weights. In the contemporary scenario, these predictions identified many of the high-occurrence areas observed in our data, although some tributaries experienced higher observed occurrence rates than our model predicted and many main-stem reaches experienced lower occurrence rates than predicted (Figure 3A, C). Likewise, differences between the predicted occurrence probabilities in the contemporary scenario versus those in the 2040 and 2080 scenarios were spatially heterogeneous (Figure 3B, D). Increases in redd occurrence probability were predicted among the furthest upstream reaches of the surveyed area, and progressive declines in occurrence probability were predicted along the lower main stem and higher-order tributaries compared to current conditions, with effects becoming more pronounced from 2040 to 2080 (Figure 3). Interestingly, some of the habitats with the largest observed contemporary redd occurrences (e.g., Bear Valley Creek, the furthest southwest tributary on the maps) were predicted to have lower occurrence probabilities in 2040 and 2080.

The predicted effects of climate change were, overall, fairly small, with H_T increasing slightly in 2040 but decreasing by 2080 (Figure 4). Decreases in H_T were most pronounced at low to mid-elevations (and distances), but upstream reach-level occurrence probabilities tended to increase under future climate scenarios, somewhat compensating for downstream losses. The variation in H_T caused by variation in fire effects was small at low elevations (and distance) but increased with increasing elevation (and distance) such that the effects of both of our climate change scenarios on whole-basin H_T fell within the range expected for contemporary interannual fire variability. However, it should be emphasized that the fire-related

uncertainty in redd occurrence depicted in Figure 4 is cumulative, such that (1) the difference between high and low bounds necessarily increases across the x-axis and (2) weaker (or stronger) fire effects of individual reaches slow (or accelerate) that increase. The close proximity of terminal H_T values for all scenarios in Figure 4 (i.e., within the range of cumulative uncertainty in the contemporary scenario due to fire) suggests that the basinwide effects of climate-driven changes in stream temperature and streamflow could be eclipsed by slight changes in fire regime.

DISCUSSION

Chinook Salmon redd occurrence was influenced by hydrogeomorphic features, streamflow, stream temperature, conspecific abundance of spawning Chinook Salmon, and fire dynamics across the MFSR, a large watershed of highly connected stream reaches that are minimally influenced by anthropogenic activities. The effects of stream temperature and stream size were modest compared to the effects of substrate size and valley confinement. Furthermore, our analyses indicated that variation in fire extent may be more influential than the moderate changes in stream temperature and flow conditions expected with climate change. Given that the extent and severity of wildfires in the study area will likely continue to increase under a warming climate (Westerling et al. 2006), post-fire increases in sediment yield and wood recruitment may be the dominant effects of future climate change on Chinook Salmon spawning habitats in the MFSR, with relatively little effect of changes in stream temperature and streamflow during the spawning period. However, climate-driven changes in streamflow variables that were not considered in our analysis, such as scour regime during embryo incubation, could affect Chinook Salmon habitat in the basin (Goode et al. 2013). These possible effects warrant further investigation.

Time-Invariant Effects

In our top models, substrate size and valley confinement strongly affected Chinook Salmon redd occurrence and interacted with other variables to further influence redd occurrence (Table 2). We observed a strongly unimodal relationship between redd occurrence and substrate size, indicating an optimal intermediate value. However, the optimal substrate size (D_{50} = 25 mm) was near the bottom of the range of preferred sizes reported in the literature for large-bodied salmonids (Kondolf and Wolman 1993). One might expect that small, marginal substrate sizes might be tolerated in unconfined valleys due to other ecological benefits (Supplement S1), but we found that redd occurrence probability was highest at D_{50} = 25 mm in both unconfined and confined valleys (Figure 2E, F). We are unsure why the fish consistently selected reaches with small substrate sizes, particularly in confined valleys, which magnify flood flows compared to unconfined floodplain rivers (Baxter and Hauer 2000; Goode et al. 2013) and should therefore elevate the scour risk of incubating embryos. However, our use of reach-average median substrate size neglects substrate size variation (Riebe et al. 2014) and the occurrence of textural patches within a reach (Buffington et al. 2004). Consequently, redds in the study area may be within patches with a larger substrate size than was indicated by the reach-scale prediction of D_{50}.

Temperature

Our results indicated an optimum stream temperature of around 14°C but little effect of interannual temperature variation (Figure 2A), suggesting that average stream temperature is a stronger control on redd occurrence or that natal homing constrains the response to interannual variability. This may seem unsurprising because the SD of interannual temperature among years was only 0.5°C; however, even small changes in mean temperature can strongly affect the timing of intra-annual temperature variation. Salmon populations are generally thought to respond to temperature variation by changing the timing of spawning (Heggberget 1988; Schindler et al. 2010) rather than by changing location, which would be consistent with our observations. Isaak et al. (2017) found no strong negative effect of high stream temperature (up to 22°C) on Chinook Salmon occurrence, possibly due to wide intra-annual variation in temperatures that allowed most streams to experience optimal spawning temperatures but at different times of the year. Our results suggest a decline in occupancy probability in reaches with mean August stream temperatures less than 12°C or greater than 16°C in the MFSR; however, the uncertainty in this relationship is high, especially at warmer temperatures (Figure 2A). If optimal thermal conditions occur at some point during the spawning season, mean August temperature may be less important than phenology or other physical variables, such as substrate, water depth, and velocity, for determining where females excavate redds (Lisi et al. 2013).

Flow

Average stream discharge in the Pacific Northwest is predicted to decline with climate change, mostly due to changes in precipitation patterns and reduced snowpack (Hamlet et al. 2013). However, predictions for the study area are more nuanced; the magnitude of high flows is expected to increase with climate change, while the magnitude of summer low flows is predicted to decline (Goode et al. 2013). Our results suggested that even within the

surveyed network, where all streams are thought to be accessible by Chinook Salmon, the lowest discharge (smallest) streams are less likely to be occupied by spawning fish (Figure 2D). Furthermore, the climate projections used in our analysis predicted declines in mean summer discharge that were too small to reduce occurrence probabilities appreciably among the smaller upstream tributaries in our network (Figures 3 and 4). However, we did not consider intra-annual variation in discharge, which might differentially affect early arriving Chinook Salmon spawners. Likewise, we did not consider the number and severity of scouring flow events during the winter egg incubation period, which are expected to increase under climate change scenarios, with negative effects for fall-spawning salmonids (Wenger et al. 2010; Goode et al. 2013).

Fire

Our work supports a growing body of literature showing the benefits of high-quality, highly connected habitats and natural fire regimes for salmon. Fire is integral to the shifting habitat mosaic concept in large rivers (Kleindl et al. 2015), which drives riverine habitat patch dynamics in space and time (Stanford et al. 2005). Natural fire regimes have an overall positive effect on Pacific salmon, although there is often a mix of positive and negative effects that take time to manifest through ecological and geomorphological processes (Flitcroft et al. 2016). In the short term, effects of fire on stream ecosystems are typically negative (Minshall 2003) and our results support this, although only weakly (Figure 2B). The lack of strong negative responses to local fire in the MFSR may be a function of the "wilderness" designation that covers over 95% of the basin (and a corresponding lack of human-driven landscape alteration), resulting in a more natural fire regime that may moderate burn severity and create diverse habitat (Parks et al. 2014). Longer-term positive fire effects (Figure 2C) are likely the result of post-fire debris flows that input gravel and large wood from the surrounding landscape (Benda et al. 2003; Dunham et al. 2003; Goode et al. 2012; Flitcroft et al. 2016; Lewicki and colleagues, unpublished data). We found a stronger positive relationship between fire and Chinook Salmon redd occurrence in unconfined valleys than in confined valleys, possibly reflecting the general tendency for lower-gradient, more sinuous reaches to retain inputs of post-fire sediment and wood longer than confined valley reaches, which are relatively steeper, narrower, and less sinuous. Others have reported that post-fire sediment inputs can be routed through steep, confined valley reaches within 5–10 years (Lewicki and colleagues, unpublished data), while sediment pulses in lower-gradient, unconfined rivers may persist for decades (Megahan et al. 1980; Madej and Ozaki 1996). Nevertheless, the periodic creation of transient spawning habitat in steep, confined valleys via post-fire debris flows may be particularly important given the overall paucity of spawning habitat in such environments. During the 21 years of redd surveys evaluated here, there were documented examples of Chinook Salmon spawning in new gravel patches deposited by post-fire debris flows (R.F.T. and J.M.B., unpublished data), demonstrating a dynamic response of redd occurrence to wildfire.

Conspecific Abundance

We found that Chinook Salmon redds tend to occur in a larger number of reaches when run sizes are larger, as has been noted previously in this system (Isaak et al. 2003; Isaak and Thurow 2006). Such colonization of new habitats could be interpreted as habitat selection behavior motivated at the individual level by density-dependent competition for habitat (Fretwell and Lucas 1970). However, contemporary Chinook Salmon abundance in the MFSR is a small fraction of historical abundances, and habitat has remained abundant, high quality, and intact (Thurow et al. 2020), so intra-specific competition is not likely to be strong. As noted above, Chinook Salmon in the MFSR have also demonstrated the capacity to colonize new post-fire debris flow deposits, sometimes in locations many kilometers from the nearest prior spawning gravels (R.F.T. and J.M.B., unpublished data)—an observation that is consistent with our finding of net positive responses to fire. At currently low population densities, the positive occurrence–abundance relationship and new patch colonization observations may be the result of density-independent homing and straying behaviors. Natal homing in Pacific salmonids can lead to differentiation among populations that return to distinct areas (Schindler et al. 2010), while straying allows genetic exchange among subpopulations that can contribute to genetic diversity and metapopulation stability (Neville et al. 2007; Keefer and Caudill 2014). Interestingly, neither homing/straying nor habitat selection, each of which is a localized process, explains why whole-basin abundance of Chinook Salmon outperformed the finer-scale abundance variables. One possibility is that synchrony in redd counts among subpopulations across the MFSR (Isaak et al. 2003) yields subbasin-scale variation in salmon abundance that, for all subbasins, mirrors the variation in abundance at the whole-basin scale such that using local subbasin counts adds no explanatory power over whole-basin counts.

We have shown that interannual variation in Chinook Salmon redd occurrence across the MFSR can be explained by spatially or annually varying environmental conditions and conspecific abundance. However, intra-annual processes (e.g., phenology) are also important for salmon population dynamics and their response to environmental variation and change. Chinook Salmon life history portfolios (including spawning temperature or

spawn timing preferences) may differ substantially among subpopulations across the MFSR as they do in other systems (Ruff et al. 2011). The annual time step at which our data were collected does not capture such important intra-annual variation in the MFSR, so further investigation with additional or complementary data sets is warranted.

Life Cycle Implications

Salmon need three things: intact natal habitat (spawning and rearing), a suitable migration corridor, and a favorable estuarine and ocean environment. Over the past approximately 70 years, reduced connectivity resulting from hydropower dam construction, along with changes in the Pacific Ocean ecosystem, has proven more powerful for explaining contemporary Chinook Salmon production and escapement than natal habitat quality and abundance in the Snake River basin (Schaller et al. 2014; Crozier et al. 2019). If natal spawning habitat was the limiting factor for Chinook Salmon population growth, the MFSR should be highly productive, with abundant salmon returns and most reaches occupied, given the abundance of high-quality, connected spawning and rearing habitats in the basin. Instead, occupancy rates vary positively with abundance, suggesting that habitats are not saturated, and contemporary run sizes are estimated at less than 3% of those from the 1950s and 1960s, even as contemporary environmental conditions in the watershed remain little changed by human activity (Thurow et al. 2020). Historically, considerable effort has been directed toward supplemental stocking and improving hydrosystem passage survival, but salmon and other migratory species rely on all phases of their life cycle to persist, including spawning habitat. Our results illustrate where favorable spawning habitats are likely to exist under future climate change scenarios and how future habitat distributions may differ from contemporary conditions, thus identifying habitats that are of high conservation priority: those that are currently high quality and are likely to persist or improve under projected climate change. Importantly, effective out-of-basin management actions to improve adult escapements are needed to take advantage of existing underseeded freshwater habitat in areas like the MFSR, where such habitats are likely to remain of high quality for the foreseeable future.

ACKNOWLEDGMENTS

Continuous redd surveys were completed with the assistance of skillful helicopter pilots Will Hogan, James Pope Sr., Ron Gipe, and John Hubof. U.S. Forest Service helicopter managers assisted, and dispatch personnel on the Boise, Payette, and Salmon–Challis National Forests provided flight monitoring; IDFG biologists participated in aerial surveys since 2013. Collaborators from the USFS–RMRS, IDFG, Shoshone–Bannock Tribes, Nez Perce Tribe, and the Payette, Boise, and Salmon–Challis National Forests completed ground-based surveys. Aerial surveys were funded by USFS–RMRS, the Payette National Forest, and the Bonneville Power Administration. Geographical information systems support and review were provided by Dave Nagel (USFS–RMRS). The manuscript was improved by helpful reviews from Craig Osenberg, Trent Sutton, and two anonymous reviewers. Reference to trade names does not imply endorsement by the U.S. Government. There is no conflict of interest declared in this article.

ORCID

Gregory R. Jacobs https://orcid.org/0000-0002-3659-1581

REFERENCES

Bartón, K.2019. MuMIn: multi-model inference. R package version 1.43.6. Available: https://CRAN.R-project.org/package=MuMIn. (January 2020).

Bates, D., M. Maechler, B. Bolker, and S. Walker. 2015. Fitting linear mixed-effects models using lme4. Journal of Statistical Software [online serial] 67(1).

Baxter, C. V., and F. R. Hauer. 2000. Geomorphology, hyporheic exchange, and selection of spawning habitat by Bull Trout (*Salvelinus confluentus*). Canadian Journal of Fisheries and Aquatic Sciences 57:1470–1481.

Beechie, T., H. Moir, and G. Pess. 2008. Hierarchical physical controls on salmonid spawning location and timing. Pages 83–101 *in* D. A. Sear and P. DeVries, editors. Salmonid spawning habitat in rivers: physical controls, biological responses, and approaches to remediation. American Fisheries Society, Symposium 65, Bethesda, Maryland.

Benda, L., C. Veldhuisen, and J. Black. 2003. Debris flows as agents of morphological heterogeneity at low-order confluences, Olympic Mountains, Washington. Geological Society of America Bulletin 115:1110–1121.

Brooks, M. E., K. Kristensen, K. J. van Benthem, A. Magnusson, C. W. Berg, A. Nielsen, H. J. Skaug, M. Machler, and B. M. Bolker. 2017. glmmTMB balances speed and flexibility among packages for zero-inflated generalized linear mixed modeling. R Journal 9:378–400.

Buffington, J. M., and D. R. Montgomery. 1999. Effects of hydraulic roughness on surface textures of gravel-bed rivers. Water Resources Research 35:3507–3522.

Buffington, J. M., D. R. Montgomery, and H. M. Greenberg. 2004. Basin-scale availability of salmonid spawning gravel as influenced by channel type and hydraulic roughness in mountain catchments. Canadian Journal of Fisheries and Aquatic Sciences 61:2085–2096.

Chapman, D. W. 1988. Critical review of variables used to define effects of fines in redds of large salmonids. Transactions of the American Fisheries Society 117:1–21.

Crozier, L. G., M. M. McClure, T. Beechie, S. J. Bograd, D. A. Boughton, M. Carr, T. D. Cooney, J. B. Dunham, C. M. Greene, M. A. Haltuch, E. L. Hazen, D. M. Holzer, D. D. Huff, R. C. Johnson, C. E. Jordan, I. C. Kaplan, S. T. Lindley, N. J. Mantua, P. B. Moyle, J. M. Myers, M. W. Nelson, B. C. Spence, L. A. Weitkamp, T. H. Williams, and E. Willis-Norton. 2019. Climate vulnerability assessment for Pacific salmon and steelhead in the California Current Large Marine Ecosystem. PLoS ONE [online serial] 14:e0217711.

Dunham, J. B., M. K. Young, R. E. Gresswell, and B. E. Rieman. 2003. Effects of fire on fish populations: landscape perspectives on persistence of native fishes and nonnative fish invasions. Forest Ecology and Management 178:183–196.

Eidenshink, J., B. Schwind, K. Brewer, Z. L. Zhu, B. Quayle, and S. Howard. 2007. A project for monitoring trends in burn severity. Fire Ecology 3:3–21.

Elith, J., and J. R. Leathwick. 2009. Species distribution models: ecological explanation and prediction across space and time. Annual Review of Ecology, Evolution, and Systematics 40:677–697.

Falcy, M. R. 2015. Density-dependent habitat selection of spawning Chinook Salmon: broad-scale evidence and implications. Journal of Animal Ecology 84:545–553.

Fausch, K. D., C. E. Torgersen, C. V. Baxter, and H. W. Li. 2002. Landscapes to riverscapes: bridging the gap between research and conservation of stream fishes: a continuous view of the river is needed to understand how processes interacting among scales set the context for stream fishes and their habitat. BioScience 52:483–498.

Flitcroft, R. L., J. A. Falke, G. H. Reeves, P. F. Hessburg, K. M. McNyset, and L. E. Benda. 2016. Wildfire may increase habitat quality for spring Chinook Salmon in the Wenatchee River subbasin, WA, USA. Forest Ecology and Management 359:126–140.

Fox, J., and G. Monette. 1992. Generalized collinearity diagnostics. Journal of the American Statistical Association 87:178–183.

Fretwell, S. D., and H. L. Lucas Jr. 1970. On territorial behavior and other factors influencing habitat distribution in birds. I. Theoretical development. Acta Biotheoretica 19:16–36.

Goode, J. R., J. M. Buffington, D. Tonina, D. J. Isaak, R. F. Thurow, S. Wenger, D. Nagel, C. Luce, D. Tetzlaff, and C. Soulsby. 2013. Potential effects of climate change on streambed scour and risks to salmonid survival in snow-dominated mountain basins. Hydrological Processes 27:750–765.

Goode, J. R., C. H. Luce, and J. M. Buffington. 2012. Enhanced sediment delivery in a changing climate in semi-arid mountain basins: implications for water resource management and aquatic habitat in the northern Rocky Mountains. Geomorphology 139:1–15.

Greig, S. M., D. A. Sear, and P. A. Carling. 2007. A review of factors influencing the availability of dissolved oxygen to incubating salmonid embryos. Hydrological Processes 21:323–334.

Hamlet, A. F., M. M. Elsner, G. S. Mauger, S. Y. Lee, I. Tohver, and R. A. Norheim. 2013. An overview of the Columbia Basin Climate Change Scenarios Project: approach, methods, and summary of key results. Atmosphere-Ocean 51:392–415.

Hartig, F. 2019. DHARMa: residual diagnostics for hierarchical (multi-level/mixed) regression models. R package version 0.2.4. Available: https://CRAN.R-project.org/package=DHARMa. (January 2020).

Heggberget, T. G. 1988. Timing of spawning in Norwegian Atlantic Salmon (*Salmo salar*). Canadian Journal of Fisheries and Aquatic Sciences 45:845–849.

Hill, R. A., M. H. Weber, S. G. Leibowitz, A. R. Olsen, and D. J. Thornbrugh. 2016. The Stream-Catchment (StreamCat) Dataset: a database of watershed metrics for the conterminous United States. Journal of the American Water Resources Association 52:120–128.

ICTRT (Interior Columbia Basin Technical Recovery Team). 2003. Independent populations of Chinook, steelhead, and Sockeye for listed evolutionarily significant units within the Interior Columbia River domain: working draft. National Marine Fisheries Service, Portland, Oregon.

IPCC (Intergovernmental Panel on Climate Change). 2007. Climate change 2007. Contribution of Working Groups I, II and III to the Fourth Assessment Report of the Intergovernmental Panel on Climate Change. IPCC, Geneva, Switzerland.

Isaak, D. J., C. H. Luce, D. L. Horan, G. L. Chandler, S. P. Wollrab, and D. E. Nagel. 2018. Global warming of salmon and trout rivers in the northwestern U.S.: road to ruin or path through purgatory? Transactions of the American Fisheries Society 147:566–587.

Isaak, D. J., and R. F. Thurow. 2006. Network-scale spatial and temporal variation in Chinook Salmon (*Oncorhynchus tshawytscha*) redd distributions: patterns inferred from spatially continuous replicate surveys. Canadian Journal of Fisheries and Aquatic Sciences 63:285–296.

Isaak, D. J., R. F. Thurow, B. E. Rieman, and J. B. Dunham. 2003. Temporal variation in synchrony among Chinook Salmon (*Oncorhynchus tshawytscha*) redd counts from a wilderness area in central Idaho. Canadian Journal of Fisheries and Aquatic Sciences 60:840–848.

Isaak, D. J., S. J. Wenger, E. E. Peterson, J. M. Ver Hoef, D. E. Nagel, C. H. Luce, S. W. Hostetler, J. B. Dunham, B. B. Roper, S. P. Wollrab, and G. L. Chandler. 2017. The NorWeST summer stream temperature model and scenarios for the western US: a crowd-sourced database and new geospatial tools foster a user community and predict broad climate warming of rivers and streams. Water Resources Research 53:9181–9205.

Isaak, D. J., M. K. Young, C. H. Luce, S. W. Hostetler, S. J. Wenger, E. E. Peterson, J. M. Ver Hoef, M. C. Groce, D. L. Horan, and D. E. Nagel. 2016. Slow climate velocities of mountain streams portend their role as refugia for cold-water biodiversity. Proceedings of the National Academy of Sciences of the United States of America 113:4374–4379.

Jensen, D. W., E. A. Steel, A. H. Fullerton, and G. R. Pess. 2009. Impact of fine sediment on egg-to-fry survival of Pacific salmon: a meta-analysis of published studies. Reviews in Fisheries Science 17:348–359.

Jolly, W. M., M. A. Cochrane, P. H. Freeborn, Z. A. Holden, T. J. Brown, G. J. Williamson, and D. M. Bowman. 2015. Climate-induced variations in global wildfire danger from 1979 to 2013. Nature Communications 6:7537.

Keefer, M. L., and C. C. Caudill. 2014. Homing and straying by anadromous salmonids: a review of mechanisms and rates. Reviews in Fish Biology and Fisheries 24:333–368.

Kleindl, W. J., M. C. Rains, L. A. Marshall, and F. R. Hauer. 2015. Fire and flood expand the floodplain shifting habitat mosaic concept. Freshwater Science 34:1366–1382.

Kondolf, G. M., and M. G. Wolman. 1993. The sizes of salmonid spawning gravels. Water Resources Research 29:2275–2285.

Leasure, D. R. 2014. Applications of a new geodata crawler for landscape ecology: from mapping natural stream hydrology to monitoring endangered beetles. Doctoral dissertation. University of Arkansas, Fayetteville.

Lee, K. N. 1997. Sustaining salmon: three principles. Pages 665–675 *in* D. J. Stouder, P. A. Bisson, and R. J. Naiman, editors. Pacific salmon and their ecosystems. Springer, Boston.

Lisi, P. J., D. E. Schindler, K. T. Bentley, and G. R. Pess. 2013. Association between geomorphic attributes of watersheds, water temperature, and salmon spawn timing in Alaskan streams. Geomorphology 185:78–86.

Luce, C. H., J. T. Abatzoglou, and Z. A. Holden. 2013. The missing mountain water: slower westerlies decrease orographic enhancement in the Pacific Northwest USA. Science 342:1360–1364.

Lynch, A. J., B. J. Myers, C. Chu, L. A. Eby, J. A. Falke, R. P. Kovach, T. J. Krabbenhoft, T. J. Kwak, J. Lyons, C. P. Paukert, and J. E. Whitney. 2016. Climate change effects on North American inland fish populations and assemblages. Fisheries 41:346–361.

Madej, M. A., and V. Ozaki. 1996. Channel response to sediment wave propagation and movement, Redwood Creek, California, USA. Earth Surface Processes and Landforms 21:911–927.

McKean, J., and D. Tonina. 2013. Bed stability in unconfined gravel bed mountain streams: with implications for salmon spawning viability in future climates. Journal of Geophysical Research: Earth Surface 118:1227–1240.

Megahan, W. F., W. S. Platts, and B. Kulesza. 1980. Riverbed improves over time: South Fork Salmon. Pages 380–395 *in* American Society of Civil Engineers, editors. Symposium on watershed management. American Society of Civil Engineers, New York.

Minshall, G. W. 2003. Responses of stream benthic macroinvertebrates to fire. Forest Ecology and Management 178:155–161.

Minshall, G. W., D. A. Andrews, J. T. Brock, C. T. Robinson, and D. E. Lawrence. 1990. Changes in wild trout habitat following forest fire. Pages 111–127 *in* F. Richardson and R. H. Hamre, editors. Wild trout IV: proceedings of the symposium. Wild Trout Symposium, Bozeman, Montana.

Moir, H. J., C. N. Gibbins, C. Soulsby, and J. H. Webb. 2006. Discharge and hydraulic interactions in contrasting channel morphologies and their influence on site utilization by spawning Atlantic Salmon (*Salmo salar*). Canadian Journal of Fisheries and Aquatic Sciences 63:2567–2585.

Montgomery, D. R., E. M. Beamer, G. R. Pess, and T. P. Quinn. 1999. Channel type and salmonid spawning distribution and abundance. Canadian Journal of Fisheries and Aquatic Sciences 56:377–387.

Montgomery, D. R., J. M. Buffington, N. P. Peterson, D. Schuett-Hames, and T. P. Quinn. 1996. Stream-bed scour, egg burial depths, and the influence of salmonid spawning on bed surface mobility and embryo survival. Canadian Journal of Fisheries and Aquatic Sciences 53:1061–1070.

Nagel, D. E., J. M. Buffington, S. L. Parkes, S. Wenger, and J. R. Goode. 2014. A landscape scale valley confinement algorithm: delineating unconfined valley bottoms for geomorphic, aquatic, and riparian applications. U.S. Forest Service General Technical Report RMRS-GTR-321.

Nagel, D., S. Wollrab, S. Parkes-Payne, E. Peterson, D. Isaak, and J. Ver Hoef. 2017. National Stream Internet hydrography datasets for spatial-stream-network (SSN) analysis. U.S. Forest Service, Rocky Mountain Research Station, Data Archive, Fort Collins, Colorado. Available: https://www.fs.fed.us/rm/boise/AWAE/projects/NationalStreamInternet/NSI_network.html. (October 2020).

Nakagawa, S., P. C. Johnson, and H. Schielzeth. 2017. The coefficient of determination R^2 and intra-class correlation coefficient from generalized linear mixed-effects models revisited and expanded. Journal of the Royal Society Interface 14:20170213.

Neville, H., D. Isaak, R. Thurow, J. Dunham, and B. Rieman. 2007. Microsatellite variation reveals weak genetic structure and retention of genetic variability in threatened Chinook Salmon (*Oncorhynchus tshawytscha*) within a Snake River watershed. Conservation Genetics 8:133–147.

NOAA (National Oceanic and Atmospheric Administration). 1992. Endangered and threatened species; threatened status for Snake River spring/summer Chinook Salmon, threatened status for Snake River fall Chinook Salmon. Federal Register 50:227(April 22, 1992): 14653–14663.

NPCC (Northwest Power and Conservation Council). 2019. 2018 Columbia River Basin Fish and Wildlife Program costs report. NPCC, Document 2019-5, Portland, Oregon.

NRC (National Research Council). 1996. Upstream: salmon and society in the Pacific Northwest. National Academies Press, Washington, D.C.

Parks, S. A., C. Miller, C. R. Nelson, and Z. A. Holden. 2014. Previous fires moderate burn severity of subsequent wildland fires in two large western US wilderness areas. Ecosystems 17:29–42.

Peterson, D. P., S. J. Wenger, B. E. Rieman, and D. J. Isaak. 2013. Linking climate change and fish conservation efforts using spatially explicit decision support tools. Fisheries 38:112–127.

R Core Team. 2019. R: a language and environment for statistical computing. R Foundation for Statistical Computing, Vienna.

Richter, A., and S. A. Kolmes. 2005. Maximum temperature limits for Chinook, Coho, and Chum salmon, and steelhead trout in the Pacific Northwest. Reviews in Fisheries Science 13:23–49.

Riebe, C. S., L. S. Sklar, B. T. Overstreet, and J. K. Wooster. 2014. Optimal reproduction in salmon spawning substrates linked to grain size and fish length. Water Resources Research 50:898–918.

Roberts, D. R., V. Bahn, S. Ciuti, M. S. Boyce, J. Elith, G. Guillera-Arroita, S. Hauenstein, J. J. Lahoz-Monfort, B. Schröder, W. Thuiller, and D. I. Warton. 2017. Cross-validation strategies for data with temporal, spatial, hierarchical, or phylogenetic structure. Ecography 40:913–929.

Roper, B. B., W. C. Saunders, and J. V. Ojala. 2019. Did changes in western federal land management policies improve salmonid habitat in streams on public lands within the interior Columbia River basin? Environmental Monitoring and Assessment 191:574.

Ruff, C. P., D. E. Schindler, J. B. Armstrong, K. T. Bentley, G. T. Brooks, G. W. Holtgrieve, M. T. McGlauflin, C. E. Torgersen, and J. E. Seeb. 2011. Temperature-associated population diversity in salmon confers benefits to mobile consumers. Ecology 92:2073–2084.

Schaller, H. A., C. E. Petrosky, and E. S. Tinus. 2014. Evaluating river management during seaward migration to recover Columbia River stream-type Chinook Salmon considering the variation in marine conditions. Canadian Journal of Fisheries and Aquatic Sciences 71:259–271.

Schindler, D. E., R. Hilborn, B. Chasco, C. P. Boatright, T. P. Quinn, L. A. Rogers, and M. S. Webster. 2010. Population diversity and the portfolio effect in an exploited species. Nature 465:609–612.

Seaber, P. R., F. P. Kapinos, and G. L. Knapp. 1987. Hydrologic unit maps. U.S. Geological Survey Water-Supply Paper 2294.

Stanford, J. A., M. S. Lorang, and F. R. Hauer. 2005. The shifting habitat mosaic of river ecosystems. Internationale Vereinigung für Theoretische und Angewandte Limnologie: Verhandlungen 29:123–136.

Thurow, R. F. 2000. Dynamics of Chinook Salmon populations within Idaho's Frank Church Wilderness: implications for persistence. Pages 143–151 *in* S. F. McCool, D. N. Cole, W. T. Borrie, J. O'Loughlin, editors. Wilderness science in a time of change conference, volume 3. U.S. Forest Service, Proceedings RMRS-P-15-VOL 3, Ogden, Utah.

Thurow, R. F., T. Copeland, and B. N. Oldemeyer. 2020. Wild salmon and the shifting baseline syndrome: application of archival and contemporary redd counts to estimate historical Chinook Salmon (*Oncorhynchus tshawytscha*) production potential in the central Idaho wilderness. Canadian Journal of Fisheries and Aquatic Sciences 77:651–665.

Tonina, D., and J. M. Buffington. 2009. A three-dimensional model for analyzing the effects of salmon redds on hyporheic exchange and egg-pocket habitat. Canadian Journal of Fisheries and Aquatic Sciences 66:2157–2153.

USGS (U.S. Geological Survey). 2006. National Elevation Dataset. Available: http://ned.usgs.gov/. (January 2020).

USGS (U.S. Geological Survey). 2010. National Hydrography Dataset. Available: http://nhd.usgs.gov/index.html. (January 2020).

Wenger, S. J., D. J. Isaak, C. H. Luce, H. M. Neville, K. D. Fausch, J. B. Dunham, D. C. Dauwalter, M. K. Young, M. M. Elsner, B. E. Rieman, and A. F. Hamlet. 2011. Flow regime, temperature, and biotic interactions drive differential declines of trout species under climate change. Proceedings of the National Academy of Sciences of the United States of America 108:14175–14180.

Wenger, S. J., C. H. Luce, A. F. Hamlet, D. J. Isaak, and H. M. Neville. 2010. Macroscale hydrologic modeling of ecologically relevant flow metrics. Water Resources Research 46:W09513.

Wenger, S. J., N. A. Som, D. C. Dauwalter, D. J. Isaak, H. M. Neville, C. H. Luce, J. B. Dunham, M. K. Young, K. D. Fausch, and B. E. Rieman. 2013. Probabilistic accounting of uncertainty in forecasts of

species distributions under climate change. Global Change Biology 19:3343–3354.

Westerling, A. L., H. G. Hidalgo, D. R. Cayan, and T. W. Swetnam. 2006. Warming and earlier spring increase western U.S. forest wildfire activity. Science 313:940–943.

SUPPORTING INFORMATION

Additional supplemental material may be found online in the Supporting Information section at the end of the article.